Indian J. Phys. **82 (4)** 415-434 (2008)

IJP

Radiation and dissipation effect on unsteady MHD micropolar flow past an infinite vertical plate in porous medium with time dependent suction

Mohamed M Abdelkhalek

Nuclear Physics Department, Nuclear Research Centre, Atomic Energy Authority, Cairo, Egypt, 13759

E-mail mohamed_moustafa_2000@yahoo com

Received 10 January 2007, accepted 15 January 2008

Abstract : An analysis is presented to study the effect of radiation on magnetohydrodynamic mixed convective unsteady laminar boundary layer flow of an optically thick electrically conducting viscous micropolar fluid past an infinite vertical plate. A uniform magnetic field is applied perpendicular to the plate By taking the radiation heat flux in the differential form, and imposing an oscillatory time-dependent perturbation, the coupled nonlinear problem is solved for the angular velocity, temperature and velocity profiles It is observed that, when the radiation parameter increases the velocity and temperature decrease in the boundary layer, whereas when Grashof number increases the velocity increases. As the magnetic parameter increases, the velocity and microrotation decrease The magnetic field can be used effectively for controlling the rate of heat transfer as required in magnetohydrodynamic applications like MHD generators, nuclear reactors, where it is used to control enormous temperature In comparison with the Newtonian fluid, the micropolar fluids have considerably different features from the Newtonian fluid in Nusselt numbers wall skin friction and wall couple stress

Keywords : Magnetohydrodynamic, micropolar flow, heat transfer, numerical analysis

PACS Nos. : 44.25.+f, 44.05.+e, 47.27 Te

1. Introduction

Micropolar fluids are fluids with microstructure belonging to a class of fluid with non-symmetrical stress tensor referred to as polar fluids. Physically they represent fluids consisting of randomly oriented particles suspended in a viscous medium. The classical theories of continuum mechanics are in adequate to explicate the microscopic manifestations of microscopic events; a new stage in the evolution of fluid dynamic theory is in progress. Eringen presented the earliest formulation of a general theory of fluid micro continua taking into account the inertial characteristics of the substructure particles, which are allowed to undergo rotation. Eringen's actual theory of a fluid

micro continuum was presented in 1964 in his paper on simple micro fluids [1]. This theory has been extended by Eringen [2] to take into account thermal effects. The theory of micropolar fluids and its extension thermo-micropolar fluids [3] may form suitable non-Newtonian fluid models which can be used to explain the flow of colloidal fluids, liquid crystals, polymeric suspensions, animal blood, *etc.*

The present problem finds application in MHD generators with neutral fluid seeding in the form of rigid micro-inclusions. Also, many industrial applications involve fluids as a working medium, and in such applications nuclear fluids are rule and clean fluids exception. The porous media heat transfer problems have several practical engineering applications such as geothermal systems, crude oil extraction and ground water pollution. Hassanien [4] investigated boundary layer flows and heat transfer on continuous accelerated sheet extruded in an ambient micropolar fluid. Several classes of different solutions of micropolar fluids have been obtained by various investigators [5,6]. The boundary layer flow of micropolar fluid has been studied by Peddieson and Mcnitt [7] through a finite difference scheme. Ahmadi [8] has studied the boundary layer flow of a micropolar fluid over a semi-infinite plate. He obtained a self-similar solution with a constant micro-inertia. Nath [9,10] has obtained similar and non-similar solutions of boundary layer equations of micropolar fluids. Gorla [11] has studied the similar solution of micropolar boundary layer flow at a stagnation point on a moving wall. Rajagopal *et al* [12] studied a boundary layer flow of a non-Newtonian over a stretching sheet with a uniform free stream. Hady [13] studied the solution of a heat transfer to a micropolar fluid from a non-isothermal stretching sheet with injection. Na and Pop [14] investigated the boundary layer flow of a micropolar fluid due to a stretching wall. Hassanien *et al* [15] studied the numerical solution for heat transfer in a micropolar fluid over a stretching sheet. Desseaux and Kelson [16] studied a micropolar fluid bounded by a stretching sheet. Hassanien and Gorla [17] studied the heat transfer to a micropolar fluid from a non-isothermal stretching sheet with suction and blowing in all the above studies, the authors have taken the stretching sheet to be oriented in horizontal direction. However, of late, the effects of magnetic field to the micropolar fluid problem are very important. Mansour and Gorla [18] studied the Joule heating effects on unsteady natural convection from a heated vertical in a micropolar fluid. Recently, Abo-Eldahab and Ghanim [19] studied convective heat transfer in an electrically conducting micropolar fluid at a stretching surface with uniform free stream. Siddeshwar and Pranech [20] investigated the magneto-convection in a micropolar fluid. Tien and Vafai [21] reported the extent of research on this topic and discussed the importance of the non-Darcian boundary and inertia effects that account for the presence of solid boundary and moderate velocity flow in the porous medium. The open literature is rich with references dealing with natural convection flow in porous medium (Chen and Lin [22], Bejan [23], Takhar and Pop [24], Nakayama and Koyama [25] and Singh and Tewari [26]).

The purpose of the present paper is to study the effect of radiation and dissipation on magnetohydrodynamic mixed convection unsteady laminar boundary layer flow of an electrically conducting viscous micropolar fluid past an infinite vertical plate. Numerical results are shown in tabular form and graphically for the velocity, angular velocity and temperature distributions as well as the local skin friction coefficient, wall couple stress and the local Nusselt number. Numerical results of velocity profile of micropolar fluids are compared with the corresponding flow problems for a Newtonian fluid. It is observed that when the radiation parameter increases the velocity and temperature decrease in the boundary layer, where as when Grashof number increases the velocity increases.

2. Mathematical formulation of the problem

We consider a two-dimensional unsteady flow of a laminar incompressible micropolar fluid past an infinite vertical porous plate moving steadily and subjected to a thermal radiation field. The x-axis is taken along the vertical plate with the direction opposite to the direction of the gravity, while the y-axis is taken normal to the plate. A uniform magnetic field of strength H_0 is applied normal to the plate in the y-direction which produces a magnetic effect in the x-direction. It is assumed here that the size of holes in the porous plate is much larger than a characteristic microscopic length scale of the micropolar fluid to simplify formulation of the boundary conditions. The magnetic Reynolds number is taken to be small enough so that the induced magnetic field can be neglected. Under these conditions, the governing conservation equations can be written as [28] :

$$\frac{\partial \bar{V}}{\partial \bar{y}} = 0 \tag{1}$$

$$\frac{\partial \bar{u}}{\partial \bar{t}} + \bar{V}\frac{\partial \bar{u}}{\partial \bar{y}} = (\nu + \nu_r)\frac{\partial^2 \bar{u}}{\partial \bar{y}^2} + \frac{\partial \bar{U}}{\partial \bar{t}} - \left(\frac{\mu^2 \sigma_c \bar{H}_0^2}{\rho} + \frac{\nu}{K}\right)$$

$$\times\left(\bar{u} - \bar{U}\right) + g\beta\left(\bar{T} - T_\infty\right) + 2\nu_r \frac{\partial \bar{N}}{\partial \bar{y}} \tag{2}$$

$$\frac{\partial \bar{T}}{\partial \bar{t}} + \bar{V}\frac{\partial \bar{T}}{\partial \bar{y}} = \frac{K}{\rho C_P}\left(\frac{\partial^2 \bar{T}}{\partial \bar{y}^2} - \nabla \bar{q}_{\bar{y}}\right) + \frac{\mu}{\rho C_P}\left(\frac{\partial \bar{u}}{\partial \bar{y}}\right)^2 \tag{3}$$

$$\frac{\partial^2 \bar{q}_{\bar{y}}}{\partial \bar{y}^2} - 3\alpha^2 \bar{q}_{\bar{y}} - 16\alpha\sigma T_\infty^3 \frac{\partial \bar{T}}{\partial \bar{y}} = 0 \tag{4}$$

$$\rho j\left(\frac{\partial \bar{N}}{\partial \bar{t}} + \bar{V}\frac{\partial \bar{N}}{\partial \bar{y}}\right) = \gamma \frac{\partial^2 \bar{N}}{\partial \bar{y}^2} \tag{5}$$

where, $\bar{T}_w$ is the wall temperature, T_∞ is the reference temperature, $\bar{U}$ is the dimensional free stream velocity, $(\bar{u}, \bar{V})$ are the dimensional velocity components, (x, y) are the dimensional Cartesian coordinates, $\bar{t}$ is the dimensional time, g is the acceleration due to gravity, V_0 is the dimensional suction velocity, $\bar{H}_0^2$ is the constant transverse magnetic field, K is the dimensional porosity parameter, C_P is the specific heat capacity, ρ is the fluid density, α^2 is the absorption coefficient, σ_c is the electrical conductivity, μ is the permeability, ν is the kinematic viscosity, ν_r is the kinematic rotational viscosity and β Stephan-Boltzman constant.

With the boundary conditions

$$\bar{u} = 0, \quad \bar{T} = \bar{T}_w, \quad N = -n\frac{\partial \bar{u}}{\partial \bar{y}}, \quad \bar{y} = 0$$

$$\bar{u} = \bar{U}(\bar{t}) = \bar{V}_0\left(1 + \varepsilon\, e^{i\bar{\omega}\bar{t}}\right), \quad \bar{T} = \bar{T}_\infty, \quad \bar{N} \to 0 \text{ as } \bar{y} \to \infty \tag{6a,b}$$

where, ε is the small positive parameter, $\bar{\omega}$ is the dimensional free stream frequency of oscillation. Since the medium is optically thin with relatively low density and $\alpha << 1$ the radiative heat flux given by eq. (4) in the spirit of Cogley *et al* [27] becomes :

$$\frac{\partial \bar{q}_y}{\partial \bar{y}} = 4\alpha^2(\bar{T} - \bar{T}_\infty) \tag{7a}$$

where,

$$\alpha^2 = \int_0^\infty \delta\lambda \frac{\partial B}{\partial \bar{T}} \tag{7b}$$

where, λ is the frequency, δ is the radiation absorption coefficient, B is the Planck's function, $\bar{q}_y$ is the radiative heat flux and k is the dimensional porosity parameter

Further, from eq. (1), it is clear that $\bar{V}$ is a constant or a function of time only and so we assume

$$\bar{V} = -V_0\left(1 + \varepsilon A\, e^{i\bar{\omega}\bar{t}}\right) \tag{8}$$

where, ε is small positive parameter, A is a real positive constant and $\varepsilon A << 1$, V_0 is a scale of suction velocity which has non-zero positive constant and the negative sign indicates that the suction velocity is towards the plate.

Proceeding with the analysis, we state the dimensionless quantities

$$u = \frac{\bar{u}}{U_0}, \quad y = \frac{\bar{V}_0}{\nu}\bar{y}, \quad \omega = \frac{4\nu}{\bar{V}_0^2}\bar{\omega}, \quad U = \frac{\bar{u}}{U_0}, \quad \theta = \frac{\bar{T} - T_\infty}{T_w - T_\infty},$$

$$\chi = \frac{\nu^2}{K\bar{V}_0^2}, \quad P_r = \frac{\mu C_P}{K}, \quad G_r = \frac{\nu g\beta(T_w - T_\infty)}{U_0\bar{V}_0^2}, \quad Ec = \frac{U_0^2}{C_P(T_w - T_\infty)},$$

$$R = \frac{4\alpha^2(T_w - T_\infty)}{\rho C_P K\bar{V}_0^2}, \quad M = \frac{\mu^2\sigma_C\bar{H}_0^2}{\rho\bar{V}_0^2} \tag{9}$$

where, G_r is the Grashof number, R is the radiation parameter, Ec is the Eckert number, M is the non-dimensional magnetic parameter, P_r is the Prandtl number, λ is the Darcy number and T_w is the wall temperature. Furthermore, the spin-gradient viscosity γ, which defines the relationship between the coefficients of viscosity and micro-inertia, is given by :

$$\gamma = (\mu + 0.5K)\bar{j} = \mu\bar{j}(1 + 0.5\xi); \quad \xi = \frac{K}{\mu} \tag{10}$$

where, ξ denotes the dimensionless viscosity ratio.

In view of eqs. (4), (7), (8), (9) and (10), eqs. (2) and (3) become

$$\frac{1}{4}\frac{\partial u}{\partial t} - \left(1 + \varepsilon Ae^{i\omega t}\right)\frac{\partial u}{\partial y} = \frac{1}{4}\frac{\partial U}{\partial t} + (1 + \xi)\frac{\partial^2 u}{\partial y^2} - \left(M^2 + \chi^2\right)(u - U) + G_r\theta + 2\xi\frac{\partial N}{\partial Y} \tag{11}$$

$$\frac{1}{4}P_r\frac{\partial\theta}{\partial t} - P_r\left(1 + \varepsilon Ae^{i\omega t}\right)\frac{\partial\theta}{\partial y} = \left(\frac{\partial^2}{\partial y^2} - R^2\right)\theta + P_r Ec\left(\frac{\partial u}{\partial y}\right)^2 \tag{12}$$

$$\frac{\partial N}{\partial t} - \left(1 + \varepsilon Ae^{i\omega t}\right)\frac{\partial N}{\partial y} = \frac{1}{\eta}\frac{\partial^2 N}{\partial y^2} \tag{13}$$

where, $\eta = \frac{\mu\bar{j}^*}{\gamma} = \frac{2}{2 + \xi}$. By setting the last term on the R.H.S. of eq. (11) and ξ equal to zero and ignoring eq. (13), eqs. (11) and (12) reduce to those reported by Israel-Cookey [28].

The transformed boundary conditions (6a, 6b) are then given by

$$u = 0, \quad \theta = 1, \quad N = -n\frac{\partial u}{\partial y} \text{ at } y = 0$$

$$u \to 1 + \varepsilon e^{i\omega t}, \quad \theta \to 0, \quad N \to 0 \text{ as } y \to \infty \tag{14}$$

where ε is a small value, we can use a regular perturbation expansion of the form

$$u(y, t) = u_0(y) + \varepsilon u_1(y)e^{i\omega t} \tag{15a}$$

$$\theta(y,t) = \theta_0(y) + \varepsilon\theta_1(y)e^{i\omega t} \tag{15c}$$

$$N(y,t) = N_0(y) + \varepsilon N_1(y)e^{i\omega t} \tag{15b}$$

Substituting eq. (15) in to eqs. (11)–(13), neglecting the terms of $O(\varepsilon^2)$, we obtain the following sequence of approximations

$$(1+\xi)u_{0yy} + u_{0y} - \left(M^2 + \lambda^2\right)u_0 = -\left(M^2 + \chi^2\right) - G_r\theta_0 - 2\xi N_{0y} \tag{16}$$

$$\theta_{0yy} + P_r\theta_{0y} - R^2\theta_0 = -P_r Ecu_{0y}^2 \tag{17}$$

$$N_{0yy} + \eta N_{0y} = 0 \tag{18}$$

$$(1+\xi)u_{1yy} + u_{1y} - \left(M^2 + \lambda^2 + i\omega/4\right)u_1$$

$$= -\left(M^2 + \chi^2 + i\omega/4\right) - G_r\theta_1 - 2\xi N_{1y} - Au_{0y} \tag{19}$$

$$\theta_{1yy} + P_r\theta_{1y} - \left(R^2 + i\omega P_r/4\right)\theta_1 = -2P_r Ecu_{0y}u_{1y} - P_r A\theta_{0y} \tag{20}$$

$$N_{1yy} + \eta N_{1y} - i\omega N_1 = -A\eta N_{0y} \tag{21}$$

with the boundary conditions

$$u_0 = 0, \quad u_1 = 0, \quad N_0 = -nu_{0y}, \quad N_1 = -nu_{1y}, \quad \theta_0 = 1, \quad \theta_1 = 0 \quad \text{at} \quad y = 0 \tag{22}$$

$$u_0 \to 1, \quad u_1 \to 1, \quad N_0 \to 0, \quad N_1 \to 0, \quad \theta_0 \to 0 \quad \theta_1 \to 0 \quad \text{as} \quad y \to \infty \tag{23}$$

To solve the simultaneous nonlinear coupled eqs. (16)–(23), we now assume that the viscous dissipation parameter (Eckert number E_c) is small and thus its general solution which is due to the dissipation.

$$u_0(y) = u_{01}(y) + E_c u_{02}(y), \quad u_1(y) = u_{11}(y) + E_c u_{12}(y)$$

$$\theta_0(y) = \theta_{01}(y) + E_c\theta_{02}(y), \quad \theta_1(y) = \theta_{11}(y) + E_c\theta_{12}(y)$$

$$N_0(y) = N_{01}(y) + E_c N_{02}(y), \quad N_1(y) = N_{11}(y) + E_c N_{12}(y) \tag{24}$$

Inserting these trial solutions into eqs. (16)–(23), sorting powers of E_c, and ignoring terms promotional to E_c^2, we obtain the following set of equations :

$$(1+\xi)u_{01yy} + u_{01y} - \left(M^2 + \chi^2\right)u_{01} = -\left(M^2 + \chi^2\right) - G_r\theta_{01} - 2\xi N_{01} \tag{25}$$

$$\theta_{01yy} + P_r\theta_{01y} - R^2\theta_{01} = 0 \tag{26}$$

$$N_{01yy} + \eta N_{01y} = 0 \tag{27}$$

$$(1+\xi)u_{02yy} + u_{02y} - \left(M^2 + \chi^2\right)u_{02} = -G_r\theta_{02} - 2\xi N_{02} \tag{28}$$

$$\theta_{02yy} + P_r\theta_{02y} - R^2\theta_{02} = -P_r u_{01y}^2 \tag{29}$$

$$N_{02yy} + \eta N_{02y} = 0 \tag{30}$$

$$(1+\xi)\,u_{11yy} + u_{11y} - \left(M^2 + \lambda^2 + i\omega/4\right)u_{11}$$

$$= -\left(M^2 + \chi^2 + i\omega/4\right) - G_r\theta_{11} - 2\xi N_{11y} - Au_{01y} \tag{31}$$

$$\theta_{11yy} + P_r\theta_{11y} - \left(R^2 + i\omega P_r/4\right)\theta_{11} = -P_r A\theta_{01y} \tag{32}$$

$$N_{11yy} + \eta N_{11y} - i\omega\eta N_{11} = -A\eta N_{01y} \tag{33}$$

$$(1+\xi)\,u_{12yy} + u_{12y} - \left(M^2 + \chi^2 + i\omega/4\right)u_{12} = -G_r\theta_{12} - 2\xi N_{12y} - Au_{02y} \tag{34}$$

$$\theta_{12yy} + P_r\theta_{12y} - \left(R^2 + i\omega P_r/4\right)\theta_{12} = -P_r A\theta_{02y} - 2P_r u_{01y}u_{11y} \tag{35}$$

$$N_{12yy} + \eta N_{12y} - i\omega\eta N_{21} = -A\eta N_{02y} \tag{36}$$

The boundary conditions are :

$$u_{01} = 0 = u_{02},\quad \theta_{01} = 1,\quad \theta_{02} = 0,\quad N_{01} = -nu_{01y},\quad N_{02} = -nu_{02y} \quad \text{on} \quad y = 0$$

$$u_{01} = 1,\quad u_{02} = 0,\quad \theta_{01} = 0 = \theta_{02},\quad N_{01} = 0,\quad N_{02} = 0 \quad \text{on} \quad y \to \infty \tag{37}$$

$$u_{11} = u_{12} = 0,\quad \theta_{11} = \theta_{12} = 0 \quad N_{11} = -nu_{11y},\quad N_{12} = -nu_{12y} \quad \text{on} \quad y = 0$$

$$u_{11} = 1,\quad u_{12} = 0,\quad \theta_{11} = 0,\quad \theta_{12} = 0 \quad N_{11} = 0,\quad N_{12} = 0 \quad \text{on} \quad y \to \infty \tag{38}$$

The solutions of eqs. (25)–(30) satisfying the boundary conditions (37) and eqs. (31)–(36) satisfying the boundary conditions (38) and substituting into eq. (24) and using eq (15), we obtain the angular velocity, the temperature and the velocity of the flow respectively as :

$$N(y,t) = \left(C_1 e^{-\eta y} + EC_2 e^{-ny}\right) - \varepsilon e^{i\omega t}\left(\left(d_3 e^{-a_4 y} + \frac{A\eta C_1}{i\omega}\,e^{-\eta y}\right) + E\left(d_6 e^{-a_4 y} - \frac{A\eta C_2}{i\omega}\,e^{-ny}\right)\right)$$

$$\theta(y,t) = e^{-a_1 y} + E\left(C_1 e^{-a_1 y} + b_3 e^{-2a_2 y} + b_4 e^{-2\eta y} + b_5 e^{-a_1 y} + b_6 e^{-(a_1+a_2)y}\right.$$

$$\left. + b_7 e^{-(a_1+\eta)y} + b_8 e^{-(\eta+a_2)y}\right) + \varepsilon e^{i\omega t}\left(-b_{17} e^{-a_3 y} + b_{17} e^{-a_1 y} + E\left(d_5 e^{-a_3 y}\right.\right.$$

$$\left. + b_{23} e^{-a_1 y} + b_{24} e^{-2a_2 y} + b_{25} e^{-2a_2 y} + b_{26} e^{-2a_1 y} + b_{27} e^{-(a_1+a_2)y}\right.$$

$$\left.\left. + b_{28} e^{-(a_1+\eta)y} + b_{29} e^{-(a_2+\eta)y} + b_{30} e^{-(a_3+a_2)y}\right.\right.$$

$$+b_{31}e^{(a_5+a_2)y}+b_{32}e^{-(a_4+a_2)y}+b_{33}e^{-(a_1+a_5)y}+b_{34}e^{-(a_1+a_3)y}$$

$$+b_{35}e^{-(a_1+a_4)y}+b_{36}e^{-(\eta+a_3)y}+b_{37}e^{(\eta+a_4)y}+\psi d_4e^{-(\eta+a_5)y}\Big)\Big)$$

$$u(y,t)=\Big(1+d_1e^{a_2y}+b_1e^{-a_1y}+b_2e^{-\eta y}\Big)+E\Big(d_2e^{-a_2y}+b_9e^{-a_1y}+b_{10}e^{-2a_2y}$$

$$+b_{11}e^{2\eta y}+b_{12}e^{-2a_1y}+b_{13}e^{(a_1+a_2)y}+b_{14}e^{-(a_1+\eta)y}+b_{15}e^{-(a_2+\eta)y}$$

$$+b_{16}e^{\eta y}\Big)\varepsilon e^{i\omega t}\Big(1+d_4e^{-a_5y}+b_{18}e^{-a_2y}+b_{19}e^{-a_1y}+b_{20}e^{-\eta y}$$

$$+b_{21}e^{-a_3y}+b_{22}e^{-a_4y}+E\Big(d_7e^{-a_5y}+b_{39}e^{-a_2y}+b_{40}e^{-a_1y}+b_{41}e^{-2a_2y}$$

$$+b_{42}e^{2\eta y}+b_{43}e^{-2a_1y}+b_{44}e^{-(a_1+a_2)y}+b_{45}e^{-(a_1+\eta)y}+b_{46}e^{-(a_2+\eta)y}$$

$$+b_{47}e^{\eta y}+b_{48}e^{-(a_3+a_2)y}+b_{49}e^{-a_3y}+b_{50}e^{(a_5+a_2)y}+b_{51}e^{-(a_4+a_2)y}$$

$$+b_{52}e^{-(a_5+a_1)y}+b_{53}e^{-(a_3+a_1)y}+b_{54}e^{-(a_1+a_4)y}+b_{55}e^{-(a_3+\eta)y}$$

$$+b_{56}e^{-(\eta+a_4)y}+b_{57}e^{-(\eta+a_5)y}+b_{58}e^{-a_4y}\Big)\Big)$$

where, the constants are given in Appendix.

Not only the velocity, pressure and temperature fields are interest, but also the wall shear stress τ_w and the heat flux at the wall q_w. Dimesionless the skin friction coefficient $C_f=\dfrac{\partial u}{\partial y}_{y=0}$ and the Nusselt number $Nu\,\mathrm{Re}_x^{-1}=-\dfrac{\partial\theta}{\partial y}_{y=0}$, where, $\mathrm{Re}_x^{-1}=V_0x/\nu$ is the Reynolds number.

3. Results and discussion

The formulation of the problem that accounts for the effect of Radiation on unsteady MHD micropolar fluid along an infinite heated vertical plate in a porous medium with time-dependent suction has been carried out in the preceding section. This enables us to carry out the numerical computations for the velocity, microrotation and temperature fields for various values of the flow conditions and fluid properties. Results for the skin friction and heat transfer rate results are presented in Table 1 for various values of M, G_r, n, ξ, P_r, R. Comparison between Newtonian and micropolar fluids are given in Table 2. In Figures 1–16, we have prepared some graphs of the stream wise velocity and micro-rotation as well as temperature profiles for a micropolar fluid with the fixed flow conditions and fluid properties, which are listed in the figure caption. Figures 1, 2

Table 1. Effects of variations of flow conditions and fluid properties on the coefficients of skin friction and heat transfer.

		C_{fF}	$NuRe^{-1}$
	0	4.30513	1.542226
M	0.5	2.98136	1.357077
	2	3.615423	1.42696
	5	3.934458	1.432654
	−10.0	−1.567314	1.455885
	−5.0	1.59311	1.434087
G_r	0.0	1.888497	1.424446
	5.0	3.615423	1.42696
	10.0	5.335271	1.441631
	0	3.189276	2.403134
n	0.1	3.289459	2.431761
	0.5	3.688339	2.541969
	1.0	4.181377	2.670114
	0.1	3.289459	2.431761
ξ	0.5	2.67632	2.412348
	1.0	2.167378	2.40591
	2.0	1.591142	2.384696
	0.71	3.289459	2.431761
P_r	1.0	3.192263	2.605943
	7.0	2.414157	7.567222
	10.0	2.280656	10.42942
	0.0	4.332877	0.7431459
R	0.5	4.023325	0.9926894
	1.0	3.615423	1.42696
	2.0	3.289459	2.431761

illustrate the variation of angular velocity distribution across the boundary layer against spanwise coordinate y for various values of viscosity ratio. For the case of different values of viscosity ratio, the microrotation profiles in the boundary layer are shown in Figure 1. As expected, it is observed that an increase in ξ leads to enhancement in buoyancy force. The effect of viscosity ratio on the velocity profiles is presented in Figure 2. The results show that the velocity gradient near the plate decreases as the viscosity ratio ξ increases. Also the velocity distribution across the boundary layer is lower for a Newtonian fluid, for the same flow conditions and fluid properties, as compared with a micropolar fluid, except for near the wall of the porous plate. For different values of the magnetic field parameter M, the microrotation, temperature and

Table 2. Comparison between Newtonian and micropolar fluids

	$\xi = 0$			$\xi = 1$		
Y	N	θ	u	N	θ	u
0 0	1 292328	1 015777	00055356	1353156	1 006729	00027052
0 2	1 059059	6292927	4989446	1188858	624075	3392327
0 4	8678083	3902096	76017551	1044096	3869863	557237
0 6	711031	2420622	8898312	09166367	2400194	6979486
0 8	5825303	15018788	9486413	08044819	1488884	7890285
1 0	4772188	09319036	9706693	07058489	09236789	848075
1 2	3909208	05782472	9746506	06191509	05730784	8863389
1 4	3202105	03588014	9706136	05429776	03555756	911051
1 6	26222769	02226334	9637184	04760779	02206321	9268854
1 8	21481553	0138141	8561594	04173438	01369054	9368824
2 0	1759351	008571414	9499134	0365795	00849541	9430325
2 2	1440868	005318397	9444348	03205656	0052718	946647
2 4	118	003299999	9400347	02808909	00327146	9485955
2 6	09663346	00204756	936581	0246097	00203017	9494579
2 8	07913373	001270472	933899	02155895	00125988	9496225
3 0	06480162	000788304	9318188	01888455	00078185	94935
3 2	05306415	000489129	9301938	01654404	00048521	9488165
3 4	04345188	000303496	9289057	01448618	00030112	9481394
3 6	03558025	000188315	9278629	01268614	00018687	9473971
3 8	02913419	000116846	92669965	01110905	00011597	9466414
4 0	02385565	000072501	9262556	00972746	00007197	9459056
4 2	01953326	000044986	9256034	00851725	00004466	9452103
4 4	01599386	000027913	9250133	00745726	00002777	944567
4 6	01309568	000017319	9244665	00652891	00001719	9439836
4 8	01072258	000010746	9239497	00571591	00001067	94346
5 0	008779448	000006668	9234536	00500397	00000662	9429978

velocity profiles against spanwise coordinate y are plotted in Figures 3, 4 and 5, respectively It is obvious that the effect of increasing values of magnetic field parameter results in a decreasing microrotation distribution across the boundary layer Furthermore, the results show that the values of temperature distribution on the plate are decreased as M increases. It is observed also, that the values of velocity distribution on the plate are decreased as M increases. The microrotation and velocity profiles against spanwise coordinate y for different values of Grashof number G_r are described in Figures 6 and 7, respectively. It is observed that an increase in G_r leads to a decrease in the values of microrotation distributions, but increases due to velocity due to enhancement in buoyancy force. Here, the positive value of G_r corresponds to

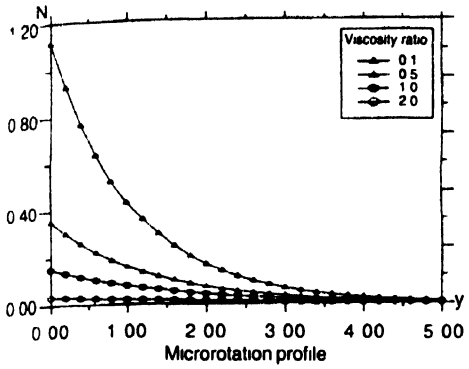

Figure 1 Microrotation profile for various values of viscosity ratio with, $\chi = 0\,5$, $n = 0\,1$, $R = 2$, $P_r = 0\,71$, $M = 2$ $Ec = 0\,01$, $A = 0\,01$, $\omega = 2$, $t = 2$, $G_r = 5$, $= 0\,1$

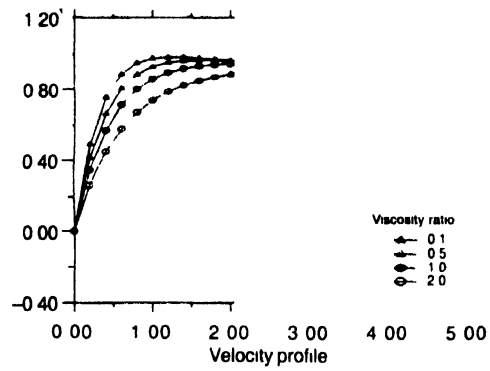

Figure 2. Velocity profile for various values ot viscosity ratio with, $\chi = 0\,5$, $n = 0\,1$, $R = 2$, $P_r = 0\,71$, $M = 2$, $Ec = 0\,01$, $A = 0\,01$ $\omega = 2$, $t = 2$ $G_r = 5$, $\varepsilon = 0\,1$

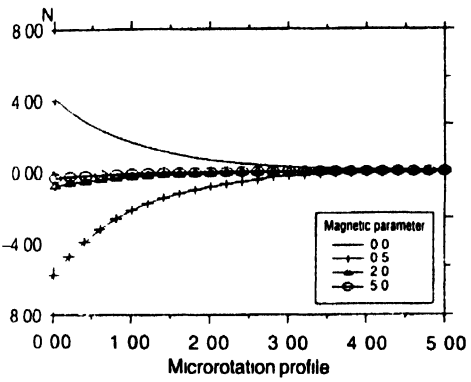

Figure 3. Microrotation profile for various values of magnetic parameter, with $\xi = 0\,1$, $\chi = 0\,5$, $n = 0\,1$, $R = 1$, $P_r = 0\,71$, $Ec = 0\,01$, $A = 0\,01$, $\omega = 2$, $t = 2$, $G_r = 5$, $\varepsilon = 0\,1$

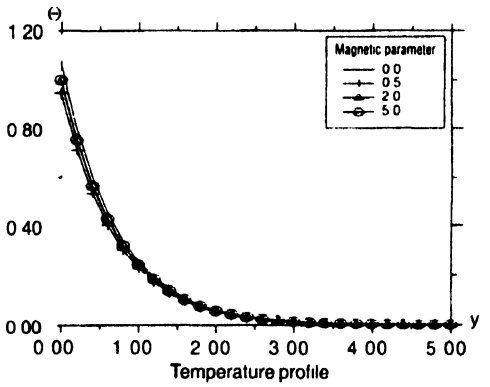

Figure 4. Temperature profile for various values of magnetic parameter, with $\xi = 0\,1$, $\chi = 0\,5$, $n = 0\,1$, $R = 1$, $P_r = 0\,71$, $Ec = 0\,01$, $A = 0\,01$, $\omega = 2$, $t = 2$, $G_r = 5$, $\varepsilon = 0\,1$

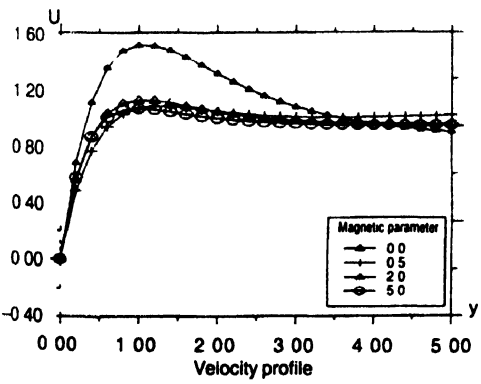

Figure 5. Velocity profile for various values ot magnetic parameter, with $\xi = 0\,1$, $\chi = 0\,5$, $n = 0\,1$, $R = 1$, $P_r = 0\,71$, $Ec = 0\,01$, $A = 0\,01$, $\omega = 2$, $t = 2$, $G_r = 5$, $= 0\,1$

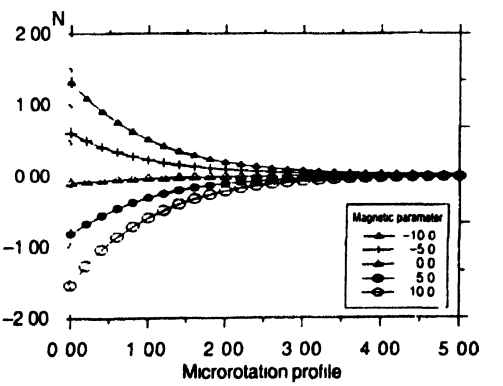

Figure 6. Microrotation profile for various values of Grashof number, with $\xi = 0\,1$, $\chi = 0\,5$, $n = 0\,1$ $R = 1$, $P_r = 0\,71$, $Ec = 0\,01$, $A = 0\,01$, $\omega = 2$, $t = 2$, $M = 2\,0$ $\varepsilon = 0\,1$

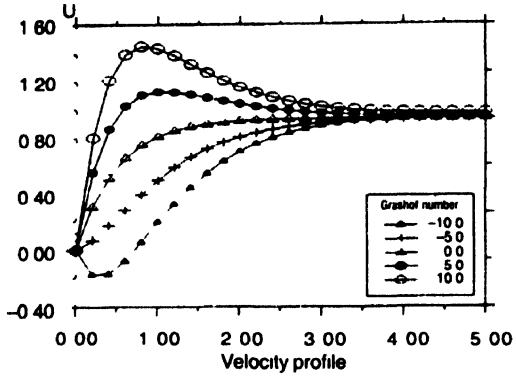

Figure 7. Velocity profile for various values of Grashof number, with $\xi = 0.1$, $\chi = 0.5$, $n = 0.1$, $R = 1$, $P_r = 0.71$, $Ec = 0.01$, $A = 0.01$, $\omega = 2$, $t = 2$, $M = 2.0$, $\varepsilon = 0.1$

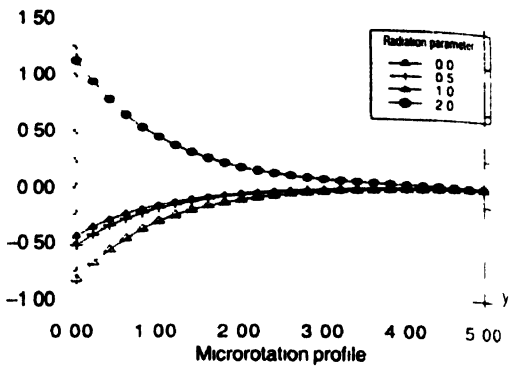

Figure 8. Microrotation profile for various values of Radiation parameter, with $\xi = 0.1$, $\lambda = 0.5$, $n = 0.1$ $M = 2$, $P_r = 0.71$, $Ec = 0.01$, $A = 0.01$, $\omega = 2$, $t = 2$ $G_r = 5$, $\varepsilon = 0.1$

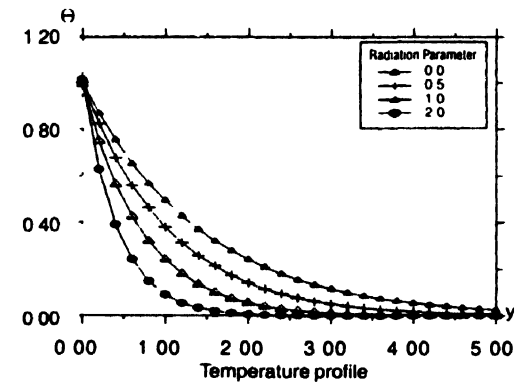

Figure 9. Temperature profile for various values of Radiation parameter, with $\xi = 0.1$, $\lambda = 0.5$, $n = 0.1$, $M = 2$, $P_r = 0.71$, $Ec = 0.01$, $A = 0.01$, $\omega = 2$, $t = 2$, $G_r = 5$, $\varepsilon = 0.1$

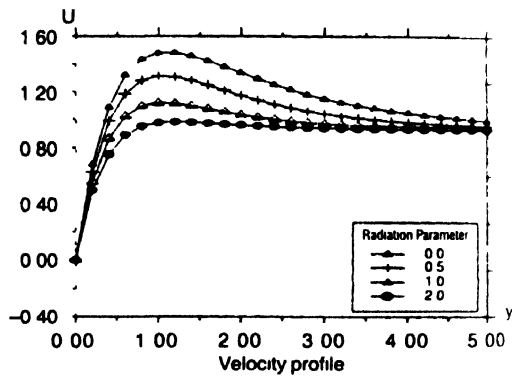

Figure 10. Velocity profile for various values of Radiation parameter, with $\xi = 0.1$, $\lambda = 0.5$, $n = 0.1$, $M = 2$ $P_r = 0.71$, $Ec = 0.01$, $A = 0.01$, $\omega = 2$, $t = 2$, $G_r = 5$ $\varepsilon = 0.1$

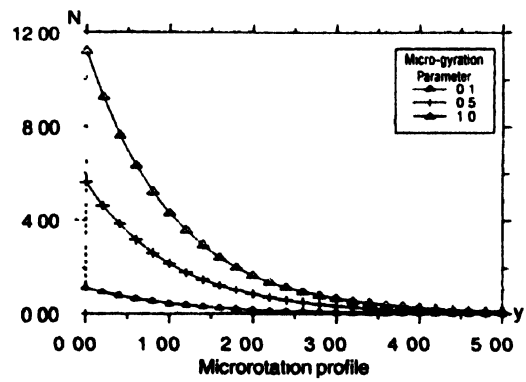

Figure 11. Microrotation profile for various values of micro-gyration parameter, with $\xi = 0.1$, $\chi = 0.5$, $R = 2.0$, $M = 2$, $P_r = 0.71$, $Ec = 0.01$, $A = 0.01$, $\omega = 2$, $t = 2$, $G_r = 5$, $\varepsilon = 0.1$.

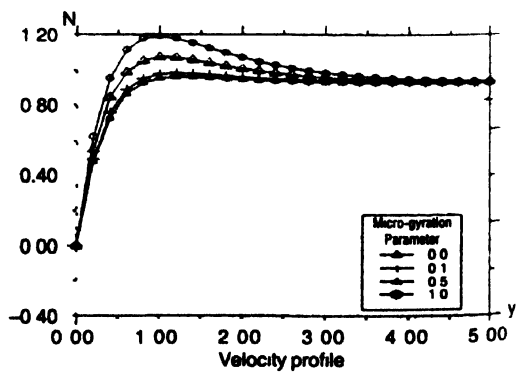

Figure 12. Velocity profile for various values of micro gyration parameter, with $\xi = 0.1$, $\chi = 0.5$, $R = 2.0$, $M = 2$, $P_r = 0.71$, $Ec = 0.01$, $A = 0.01$, $\omega = 2$, $t = 2$, $G_r = 5$, $\varepsilon = 0.1$.

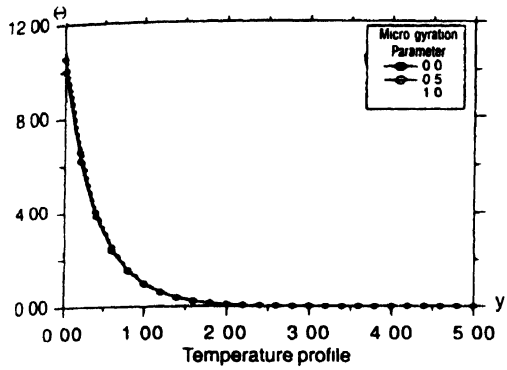

Figure 13. Temperature profile for various values of micro-gyration parameter, with $\xi = 0.1$, $\lambda = 0.5$, $R = 2.0$, $M = 2$, $P_r = 0.71$, $Ec = 0.01$, $A = 0.01$, $\omega = 2$, $t = 2$ $G_r = 5$, $\varepsilon = 0.1$

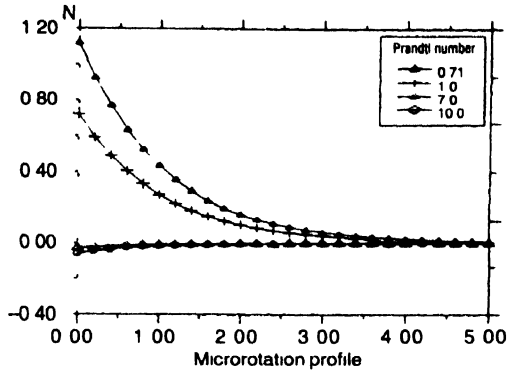

Figure 14. Microrotation profile for various values of Prandtl number, with $\xi = 0.1$, $\lambda = 0.5$, $n = 0.1$, $M = 2$, $R = 2$, $Ec = 0.01$, $A = 0.01$ $\omega = 2$ $t = 2$ $G_r = 5$, $\varepsilon = 0.1$

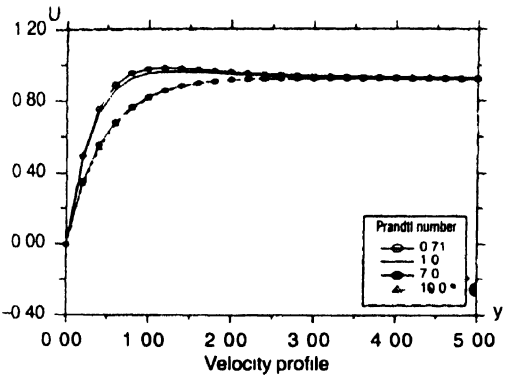

Figure 15. Velocity profile for various values of Prandtl number, with $\xi = 0.1$, $\lambda = 0.5$, $n = 0.1$, $M = 2$, $R = 2$, $Ec = 0.01$, $A = 0.01$, $\omega = 2$, $t = 2$, $G_r = 5$, $\varepsilon = 0.1$

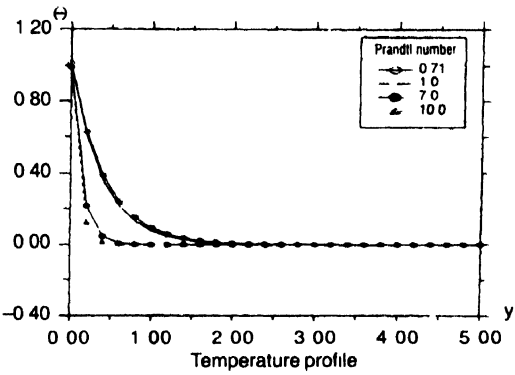

Figure 16. Temperature profile for various values of Prandtl number, with $\xi = 0.1$, $\lambda = 0.5$, $n = 0.1$, $M = 2$, $R = 2$, $Ec = 0.01$, $A = 0.01$, $\omega = 2$ $t = 2$, $G_r = 5$, $\varepsilon = 0.1$

a cooling of the surface by natural convection. In addition, the curves show that the peak value of velocity increases rapidly near the wall as the Grashof number increases and then decays to the free stream velocity. For different values of the radiation parameter R, the microrotation, temperature and velocity profiles are plotted in Figures 8, 9 and 10 respectively. It is obvious that an increase in the radiation parameter R results in decreasing velocity, microrotation and temperature within the boundary layer, as well as a decreased thickness of the velocity and temperature boundary layers. This is because the large R-values correspond to an increased dominance of conduction over radiation thereby decreasing buoyancy force and thickness of the thermal and momentum boundary layers. For the case of a micropolar fluid, the profiles of microrotation and stream wise velocity against the spanwise coordinate y for the variations of the parameter (n) in the boundary condition for micro gyration vector are shown in Figures 11 and 12 respectively. The results show that increasing values of (n) parameter results in increasing the microrotation profiles as

the n-parameter increases. However, increasing values of n-parameter results in an increasing velocity within the boundary layer, which eventually approaches to the relevant free stream velocity at the edge of boundary layer. Figure 13 depicts the temperature profiles against spanwise coordinate y for different values of micro-gyration parameter n. The numerical results show that an increase of micro-gyration parameter results an increasing thermal boundary layer thickness and more temperature distribution a cross the boundary layer. Figures 14, 15 and 16 depict the microrotation, velocity and temperature profiles against spanwise coordinate y for different values of Prandtl number P_r. The numerical results show that the effect of increasing values of Prandtl number results in a decreasing microrotation and velocity profiles and then approaches a constant value, which is relevant to the free stream velocity at the edge of boundary layer. The results also reveal that the peak value of velocity decreases as P_r decreases. Typical variations of the temperature profiles along the spanwise coordinate are shown in Figure 16 for different values of Prandtl number P_r. The numerical results show that an increase of Prandtl number results in a decreasing thermal boundary layer thickness and more uniform temperature distribution across the boundary layer. The reason is that smaller values of P_r are equivalent to increasing the thermal conductivities, and therefore heat is able to diffuse away from the heated surface more rapidly than for higher values of P_r. Hence, the boundary layer is thicker and the rate of heat transfer is reduced, for gradients have been reduced. It should be mentioned that in the absence of the micropolar fluids effects, all of the flow and heat transfer solutions reported above are consistent with those reported earlier by Israel-Cookey [28].

4. Conclusions

We have used the theory of micropolar fluids due to Eringen to formulate a set of ordinary differential governing equations for an unsteady, incompressible, laminar, micropolar fluid past an infinite vertical plate. Numerical results are presented to illustrate the details of the flow and heat transfer characteristics and their dependence on the material properties of the micropolar fluid. In a radiation dominated problem, thermal and momentum boundary layers increase in size, thereby leading to enhanced buoyancy-induced transport but decreased rate of heat transfer at the wall. We also found that there is an optimal value of radiation parameter that results in a minimum friction at the surface of the wall. From the physical point of view, $G_r > 0$ corresponds to the cooling of the plate by free convection currents and $G_r < 0$ corresponds to the heating of the plate by free convection, which agrees with the obtained results. The velocity distributions for micropolar fluids near the porous plate are less than that of Newtonian fluid, which will result in decreasing the wall shear stress. It is also noted that there exists optimal conditions for reducing skin friction on the moving porous plate. The heat transfer rate of a micropolar fluid is smaller than a Newtonian fluid, but the skin friction of a micropolar fluid is larger than a Newtonian

fluid under all circumstances As the magnetic parameter increases both the velocity and microrotation decrease. The micropolar effects behave as a coolant and are thus effective in reducing cooling rate and help in producing the desired temperature The magnetic field can be used effectively for controlling the rate of heat transfer as required in magnetohydrodynamic applications like MHD generators, nuclear reactors, where it is used to control enormous temperatures

Acknowledgments

Appreciation is extended to the referees for their constructive and helpful comments and suggestions These led to improvements in the revised paper

References

[1] A C Eringen *Int J Eng Sci* **2** 203 (1964)
[2] A C Eringen *Math Mech* **16** 1 (1966)
[3] A C Eringen *Math Anal Appl* **38** 480 (1972)
[4] I A Hassanien *Int Comm Heat Mass Transfer* **25** 571 (1998)
[5] R S R Gorla *Int J Engg Sci* **18** 611 (1980)
[6] F S Lien and C K Chen *Int J Engg Sci* **24** 991 (1986)
[7] J Peddieson and R P MCNitt *Recent Adv Engg Sci* **5** 405 (1970)
[8] G Ahmadi *Int J Engg Sci* **14** 639 (1976)
[9] G Nath *Rheol Acta* **14** 850 (1975)
[10] G Nath *Rheol Acta* **15** 209 (1976)
[11] R S R Gorla, R Pender and J Eppich *Int J Engg Sci* **21** 791 (1983)
[12] R K Rajagopal, T Y Na and A S Gupta *J Math Phys Sci* **21** 189 (1987)
[13] F M Hady *Int J Num Meth Heat Fluid Flow* **6** 6 (1997)
[14] T Y Na and I Pop *Arch Appl Mech* **67** 229 (1997)
[15] I Hassanien R S R Gorla and A A Abdulah *Appl Mech Engg* **3** 3 (1998)
[16] A Desseaux and N A Kelson *Anziam J* **42** 536 (2000)
[17] I A Hassanien and R S R Gorla *Acta Mech* **84** 1910 (1990)
[18] M A Mansour and R S R Gorla *Can J Phys* **77** 1 (1999)
[19] E M Abo-Eldahab and A F Ghonaim *Appl Math Comp* **137** 323 (2003)
[20] Pradeep G Siddheswar and S Pranech *Int J Engg Sci* **36** 1173 (1998)
[21] C I Tien and K Vafai *Adv Appl Mech* **27** 225 (1990)
[22] C Chen and C Lin *Int J Engg Sci* **33** 1233 (1993)
[23] A Bejan *Convective Heat Transfer* (1st edn) (New York Wiley) **Chap. 11** (1984)
[24] H S Takhar and I Pop *Mech Res Commun* **14** 81 (1987)
[25] A Nakayama and H Koyama *Appl Sci Res* **46** 309 (1987)
[26] P Singh and K Tewari *Int J Engg Sci* **31** 1233 (1993)
[27] A C L Cogley, W G Vincenti and E S Gilles *Am Inst Aeronaut Astronaut J* **6** 551 (1968)
[28] C Israel-Cookey, A Ogulu and V B Omubo-Pepple *Int J Heat Mass Transfer* **46** 2305 (2003)

Appendix

$$a_1 = 0.5\left(P_r + \sqrt{P_r^2 + 4R^2}\right), \quad a_2 = \frac{1+\sqrt{1+4(1+\xi)\left(M^2+\chi^2\right)}}{2(1+\xi)},$$

$$b_1 = \frac{-G_r}{\left(a_1(1+\xi)a_1 - 1\right) - \left(M^2+\lambda^2\right)}, \quad b_2 = \frac{-2\xi C_1}{\eta\left((1+\xi)\eta - 1\right) - \left(M^2+\chi^2\right)},$$

$$d_1 = -(1+b_1+b_2), \quad b_3 = \frac{P_r d_1^2 a_2^2}{2a_2(2a_2 - P_r) - R^2}, \quad b_4 = \frac{P_r b_2 \eta^2}{2\eta(2\eta - P_r) - R^2},$$

$$b_5 = \frac{P_r a_1^2 b_1^2}{2a_1(2a_1 - P_r) - R^2}, \quad b_6 = \frac{2P_r a_1 b_1 d_1 a_2}{\left((a_1+a_2)\left((a_1+a_2) - P_r\right) - R^2\right)},$$

$$b_7 = \frac{2P_r a_1 b_1 \eta b_2}{\left((a_1+\eta)\left((a_1+\eta) - P_r\right) - R^2\right)}, \quad b_8 = \frac{2P_r a_2 d_1 \eta b_2}{\left((a_2+\eta)\left((a_2+\eta) - P_r\right) - R^2\right)},$$

$$a_2 = \frac{1+\sqrt{1+4(1+\xi)\left(M^2+\chi^2\right)}}{2(1+\xi)}, \quad b_9 = \frac{G_r\sum_{i=3}^{8} b_i}{\left(a_1\left((1+\xi)a_1 - 1\right) - \left(M^2+\lambda^2\right)\right)},$$

$$b_{10} = \frac{-G_r b_3}{\left(2a_2\left((1+\xi)a_2 - 1\right) - \left(M^2+\lambda^2\right)\right)}, \quad b_{11} = \frac{-G_r b_4}{\left(2\eta\left(2(1+\xi)\eta - 1\right) - \left(M^2+\lambda^2\right)\right)}$$

$$b_{12} = \frac{-G_r b_5}{\left(2a_1\left(2(1+\xi)a_1 - 1\right) - \left(M^2+\chi^2\right)\right)}, \quad b_{13} = \frac{-G_r b_6}{\left((a_1+a_2)\left((1+\xi)(a_1+a_2) - 1\right) - \left(M^2+\lambda^2\right)\right)}$$

$$b_{14} = \frac{-G_r b_7}{\left((1+\xi)(a_1+\eta)^2 - (a_1+a_2) - \left(M^2+\lambda^2\right)\right)},$$

$$b_{15} = \frac{-G_r b_8}{\left((\eta+a_2)\left((1+\xi)(\eta+a_2) - 1\right) - \left(M^2+\chi^2\right)\right)},$$

$$b_{16} = \frac{-2\xi C_2}{\left(\eta\left((1+\eta)\eta - 1\right) - \left(M^2+\chi^2\right)\right)}, \quad d_2 = -\sum_{i=9}^{16} b_i,$$

$$a_3 = 0.5\left(P_r + \sqrt{P_r^2 + 4\left(R^2 + .25i\omega P_r\right)}\right),$$

$$b_{17} = P_r A a_1\left(a_1(a_1 - P_r) - \left(R^2 + .25i\omega P_r\right)\right)^{-1}, \quad a_4 = 0.5\left(\eta + \sqrt{\eta^2 + 4i\omega\eta}\right),$$

$$a_5 = \left(1+\sqrt{1+4(1+\xi)\left(\chi^2+M^2+.25i\omega\right)}\right)\left(2(1+\xi)\right)^{-1},$$

$$b_{18} = Ad_1a_2\left(a_2\left((1+\xi)a_2-1\right)-\left(\chi^2+M^2+.25i\omega\right)\right)^{1},$$

$$b_{19} = \frac{Ab_1a_1 - G_rb_{17}}{\left(a_1\left((1+\xi)a_1-1\right)-\left(\chi^2+M^2+.25i\omega\right)\right)},$$

$$b_{20} = \frac{i\omega Ab_2\eta + 2\xi A\eta^2C_1}{i\omega\left(\eta\left((1+\xi)\eta-1\right)-\left(\chi^2+M^2+.25i\omega\right)\right)},$$

$$b_{21} = \frac{G_rb_{17}}{\left(a_3\left((1+\xi)a_3-1\right)-\left(\chi^2+M^2+.25i\omega\right)\right)},$$

$$b_{22} = \frac{2\xi d_3a_4}{\left(a_4\left((1+\xi)a_4-1\right)-\left(\chi^2+M^2+.25i\omega\right)\right)},$$

$$d_4 = -(1+b_{18}+b_{19}+b_{20}+b_{21}+\phi_1d_2),\quad b_{23} = \frac{P_rAa_1C_1}{\left(a_1(a_1-P_r)-\left(R^2+.25i\omega P_r\right)\right)},$$

$$b_{24} = \frac{2P_ra_2\left(b_3-d_1b_{18}a_2\right)}{\left(a_2(2a_2-P_r)-\left(R^2+.25i\omega P_r\right)\right)},\quad b_{25} = \frac{2P_r\eta(b_4-b_2b_{20}\eta)}{\left(\eta(\eta-P_r)-\left(R^2+.25i\omega P_r\right)\right)},$$

$$b_{26} = \frac{2P_ra_1\left(b_5-a_1b_1b_{19}\right)}{\left(a_1(2a_1-P_r)-\left(R^2+.25i\omega P_r\right)\right)},$$

$$b_{27} = \frac{P_r\left(b_6(a_1+a_2)-2d_1a_1a_2b_{19}-2a_1a_2b_1b_{18}\right)}{\left((a_1+a_2)\left((a_1+a_2)-P_r\right)-\left(R^2+0.25i\omega\right)\right)},$$

$$b_{28} = \frac{P_r\left((a_1+\eta)b_7-2a_1b_1b_{20}\eta-2b_2a_1b_{19}\right)}{\left((a_1+\eta)\left((a_1+\eta)-P_r\right)-\left(R^2+.25i\omega\right)\right)},$$

$$b_{29}\quad \frac{P_r\left((a_2+\eta)-2d_1a_2b_{20}\eta-2b_2a_2\eta b_{18}\right)}{\left((a_1+\eta)\left((a_2+\eta)-P_r\right)-\left(R^2+.25i\omega\right)\right)},$$

$$b_{30}\quad \frac{-2P_rd_1a_2a_3b_{21}}{\left((a_2+a_3)\left((a_2+a_3)-P_r\right)-\left(R^2+.25i\omega\right)\right)},$$

$$b_{31} = \frac{-2P_r d_1 a_2 a_5 d_4}{\left((a_2 + a_5)\left((a_2 + a_5) - P_r\right) - \left(R^2 + .25i\omega P_r\right)\right)},$$

$$b_{32} = \frac{-2P_r d_1 a_2 a_4 b_{22}}{\left((a_2 + a_4)\left((a_2 + a_4) - P_r\right) - \left(R^2 + .25i\omega P_r\right)\right)},$$

$$b_{33} = \frac{-2P_r b_1 a_1 a_5 d_4}{\left(a_1 + a_5\right)\left((a_1 + a_5) - P_r\right) - \left(R^2 + .25i\omega P_r\right)\right)},$$

$$b_{34} = \frac{-2P_r a_1 b_1 a_3 b_{21}}{\left((a_1 + a_3)\left((a_1 + a_3) - P_r\right) - \left(R^2 + .25i\omega P_r\right)\right)},$$

$$b_{35} = \frac{-2P_r a_1 b_1 a_4 b_{22}}{\left((a_1 + a_4)\left((a_1 + a_4) - P_r\right) - \left(R^2 + .25i\omega P_r\right)\right)},$$

$$b_{36} = \frac{-2P_r a_3 b_{21} b_2 \eta}{\left((a_3 + \eta)\left((a_3 + \eta) - P_r\right) - \left(R^2 + .25i\omega P_r\right)\right)},$$

$$b_{37} = \frac{-2P_r a_4 b_2 \eta b_{22}}{\left((a_4 + \eta)\left((a_4 + \eta) - P_r\right) - \left(R^2 + .25i\omega P_r\right)\right)},$$

$$b_{38} = \frac{-2P_r a_5 d_4 b_2 \eta}{\left((a_5 + \eta)\left((a_5 + \eta) - P_r\right) - \left(R^2 + .25i\omega P_r\right)\right)}, \quad d_5 = -\sum_{i=23}^{37} b_i + \psi_1 d_4,$$

$$b_{39} = \frac{Aa_2 d_2}{\left(a_2\left((1+\xi)a_2 - 1\right) - \left(\chi^2 + M^2 + .25i\omega\right)\right)},$$

$$b_{40} = \frac{Aa_1 b_9 - G_r b_{23}}{\left(a_1\left((1+\xi)a_1 - 1\right) - \left(\chi^2 + M^2 + .25i\omega\right)\right)},$$

$$b_{41} = \frac{2Aa_1 b_{10} - G_r b_{24}}{\left(a_2\left((1+\xi)a_2 - 1\right) - \left(\chi^2 + M^2 + .25i\omega\right)\right)},$$

$$b_{42} = \frac{2A\eta_1 b_{11} - G_r b_{25}}{\left(\eta\left(2(1+\xi)\eta - 1\right) - \left(\chi^2 + M^2 + .25i\omega\right)\right)},$$

$$b_{43} = \frac{2Ab_{12} a_1 - G_r b_{26}}{\left(a_1\left(2(1+\xi)a_1 - 1\right) - \left(\chi^2 + M^2 + .25i\omega\right)\right)},$$

$$b_{44} = \frac{-Ab_{13}(a_1 + a_2) - G_r b_{27}}{\left((a_1 + a_2)\left((1+\xi)(a_1 + a_2) - 1\right) - \left(\lambda^2 + M^2 + .25i\omega\right)\right)},$$

$$b_{45} = \frac{Ab_{14}(a_1 + \eta) - G_r b_{28}}{\left((a_1 + \eta)\left((1+\xi)(a_1 + \eta) - 1\right) \left(\lambda^2 + M^2 + .25i\omega\right)\right)},$$

$$b_{46} = \frac{Ab_{15}(\eta + a_2) - G_r b_{29}}{\left((\eta + a_2)\left((1+\xi)(\eta + a_2) \; 1\right) - \left(\lambda^2 + M^2 + 25i\omega\right)\right)},$$

$$b_{47} = \frac{i\omega Ab_{16}\eta - 2\xi AC_2\eta^2}{i\omega\left(\eta\left((1+\xi)\eta - 1\right) - \left(\lambda^2 + M^2 + 25i\omega\right)\right)},$$

$$b_{48} = \frac{-G_r b_{30}}{\left((a_3 + a_2)\left((1+\xi)(a_3 + a_2) \; 1\right) - \left(\lambda^2 + M^2 + 25i\omega\right)\right)},$$

$$b_{49} = \frac{-G_r d_5}{\left(a_3\left((1+\xi)a_3 - 1\right) - \left(\lambda^2 + M^2 + .25i\omega\right)\right)},$$

$$b_{50} = \frac{G_r b_{31}}{\left((a_5 + a_2)\left((1+\xi)(a_5 + a_2) - 1\right) \left(\lambda^2 + M^2 + 25i\omega\right)\right)},$$

$$b_{51} = \frac{-G_r b_{32}}{\left((a_4 + a_2)\left((1+\xi)(a_4 + a_2) - 1\right) - \left(\lambda^2 + M^2 + .25i\omega\right)\right)},$$

$$b_{52} = \frac{G_r b_{33}}{\left((a_1 + a_5)\left((1+\xi)(a_1 + a_5) - 1\right) \left(\lambda^2 + M^2 + .25i\omega\right)\right)},$$

$$b_{53} = \frac{-G_r b_{34}}{\left((a_3 + a_1)\left((1+\xi)(a_3 + a_1) - 1\right) - \left(\lambda^2 + M^2 + .25i\omega\right)\right)},$$

$$b_{54} = \frac{-G_r b_{35}}{\left((a_1 + a_4)\left((1+\xi)(a_1 + a_4) - 1\right) - \left(\lambda^2 + M^2 + .25i\omega\right)\right)},$$

$$b_{55} = \frac{-G_r b_{36}}{\left((a_3 + \eta)\left((1+\xi)(a_3 + \eta) - 1\right) - \left(\lambda^2 + M^2 + .25i\omega\right)\right)},$$

$$b_{56} = \frac{-G_r b_{37}}{\left((\eta + a_4)\left((1+\xi)(\eta + a_4) - 1\right) - \left(\lambda^2 + M^2 + .25i\omega\right)\right)},$$

$$b_{57} = \frac{-G_r b_{38}}{\left((\eta + a_5)\left((1+\xi)(\eta + a_5) - 1\right) - \left(\chi^2 + M^2 + .25i\omega\right)\right)},$$

$$b_{58} = \frac{2\xi a_4 d_6}{\left(a_4\left((1+\xi)a_4 - 1\right) - \left(\chi^2 + M^2 + .25i\omega\right)\right)},$$

$$d_7 = -\sum_{i=39}^{57} b_i + \phi_2 d_6, \quad \phi_2 = \frac{2\xi a_4 d_6}{\left(a_4\left((1+\xi)a_4 - 1\right) - \left(\chi^2 + M^2 + .25i\omega\right)\right)}$$